

# Sequential Biaxial Low-Cycle Fatigue of Titanium Alloys

Sergiy Shukayev, Maksym Gladyski, Konstantyn Panasovskyi

Institute of Mechanical Engineering, National Technical University of Ukraine "Kyiv Polytechnic Institute", 37 Peremogy ave., 03056 Kyiv, Ukraine; Fax: +38 044 406 8019; E-mail: s.shukayev@kpi.ua

**ABSTRACT.** *The paper contains the results of the sequential biaxial low-cycle fatigue tests for titanium alloys BT1-0, BT9 subjected to axial loading, torsion and combined axial loading with torsion. Biaxial LCF tests were conducted under strain control. The results from the testing showed that the fatigue life for titanium alloys depends on such factors as the loading sequence, the strain path, and the stress state. The obtained lives were compared with the calculated ones with the use of a strain-path-dependent fatigue damage parameter and two cumulative damage models: Miner's linear rule and the Manson-Halford hypothesis. It has been shown that under biaxial variable loading results of LCF life calculated according to the Manson-Halford hypothesis are well correlated with the results of tests for two titanium alloys.*

## INTRODUCTION

Most engineering components during their service life are subjected to multiaxial loading, which is generally variable. Due to the inherent complexities the life estimation under multiaxial variable amplitude loading is an extremely difficult topic. At present, the fatigue data of this sort are meager.

The objective of this study is to investigate the effects of non-proportional and irregular loading on the low cycle fatigue behavior of titanium alloys BT1-0, BT9.

Titanium and its alloys widely used in aerospace engineering, chemical industry, medicine and et al. These materials have a unique set of physical, mechanical, chemical and performance properties such as the high strength, unique corrosion resistance in various environments, smallest coefficient of thermal expansion among metals and alloys, and high melting point. Knowledge about fatigue behavior of titanium alloys is necessary for the structural design.

## EXPERIMENTAL PROCEDURE

Commercially available pure titanium BT1-0 and titanium alloy BT9 as an  $\alpha + \beta$  phase wrought alloy were used in this study. Chemical compositions of both materials are presented in Table 1. Solid bars with 25 mm diameter and 100 mm length were

machined to tubular specimens of the configurations and dimensions shown in Fig. 1. The specimen geometries were designed based on the State Standard of Ukraine [1].

Table 1. Chemical compositions in percent weight for the BT1-0 and BT9 titanium alloy

Material	Fe	C	Si	Mo	N	Al	Zr	H	Ti
BT1-0	0.02	–	0.01	–	–	0.45	–	–	bal.
BT9	0.081	0.06	0.3	3.4	0.018	6.5	1.58	0.006	bal.

Axial and shear fatigue properties as well as mechanical properties for pure titanium and titanium alloy BT9 were found from monotonic and constant amplitude loading tests [2] and listed in Table 2.

Table 2. Mechanical properties, axial and shear fatigue coefficients for BT1-0 and BT9 titanium alloys

Properties	BT1-0	BT9
Modulus of elasticity, $E$ , GPa	112	118
Shear modulus, $G$ , GPa	40	43
Yield strength, $\sigma_y$ , MPa	475	910
Ultimate tensile strength, $\sigma_U$ , MPa	558	1,080
Axial fatigue strength coefficient, $\sigma'_f$ , MPa	647	1,180
Axial fatigue strength exponent, $b$	-0.033	-0.025
Axial fatigue ductility coefficient, $\epsilon'_f$	0.548	0.278
Axial fatigue ductility exponent, $c$	-0.646	-0.665
Shear fatigue strength coefficient, $\tau'_f$ , MPa	485	881
Shear fatigue strength exponent, $b_s$	-0.069	-0.082
Shear fatigue ductility coefficient, $\gamma'_f$	0.417	0.180
Shear fatigue ductility exponent, $c_s$	-0.523	-0.470

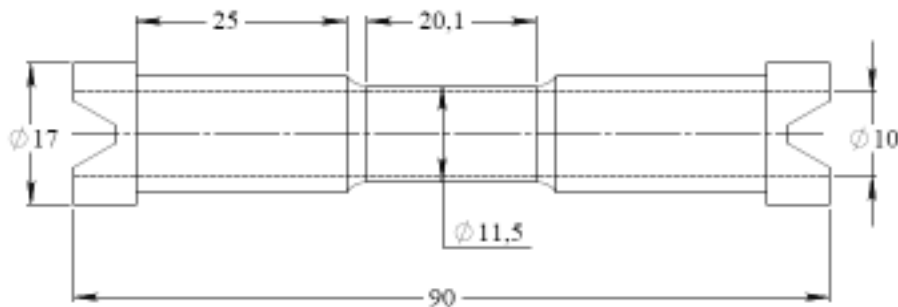


Figure 1. Tubular specimen configuration and dimensions in mm

A closed-loop mechanical drive axial-torsion load frame and a digital controller with frequency of 0.03 Hz were used for conducting all experiments in this study. The schematic description of the testing machine is presented in Fig. 2. An electric-powered drive consisting of two direct current motors was used to apply axial and torsion loading. Direct current motors were controlled by the thyristors control units (TCU), which was inter-phased by a PC through a digital-analog converter (ADC). During cyclic tests, the feedback coupling was also operated to allow following and correcting loading paths with the prescribed accuracy. Test results were recorded by X-Y plotters. All analog signals were amplified by a tension sensor unit. An axial-torsion extensometer was used to control and measure axial and shear strains.

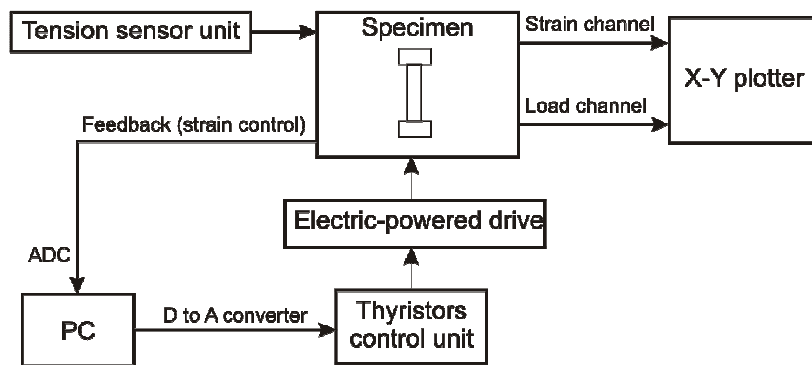


Figure 2. Principal scheme of testing machine

Axial  $\varepsilon(t)$  and shear strain  $\gamma(t)$  of the fully-reversed strain control tests were changed on sinusoidal equations as following:

$$\varepsilon_x(t) = \varepsilon_a \sin(\omega t), \gamma_{xy}(t) = \gamma_a \sin(\omega t + \theta) \quad (1)$$

where  $\varepsilon_a$  and  $\gamma_a$  are axial and shear strain amplitude respectively;  $\omega$  is angular frequency, and  $\theta$  is phase angel.

Different combinations of sinusoidal axial (path “a”,  $\gamma_a = 0$ ), torsion (path “t”,  $\varepsilon_a = 0$ ), and 90° out-of-phase (path “o”) strain paths were applied for tests shown in Fig. 3.

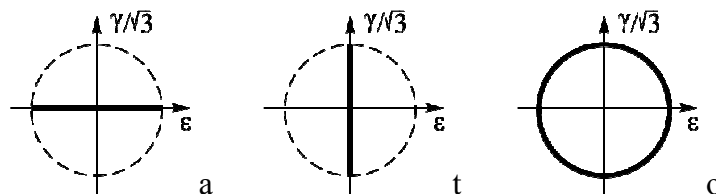


Figure 3. Axial (a), torsion (t), and 90° out-of-phase (o) strain paths used in this study

The experimental program includes the set of blocks shown on Fig. 4 under low-cycle fatigue loading by various combinations of sinusoidal strain paths and von Mises equivalent strain:

- axial or torsion loading blocks with changing of von Mises equivalent strain only (A and T blocks);
- two-stage loading blocks with constant of von Mises equivalent strain and with different strain paths (B blocks);
- loading blocks with changing both of von Mises equivalent strain and strain path (C blocks).

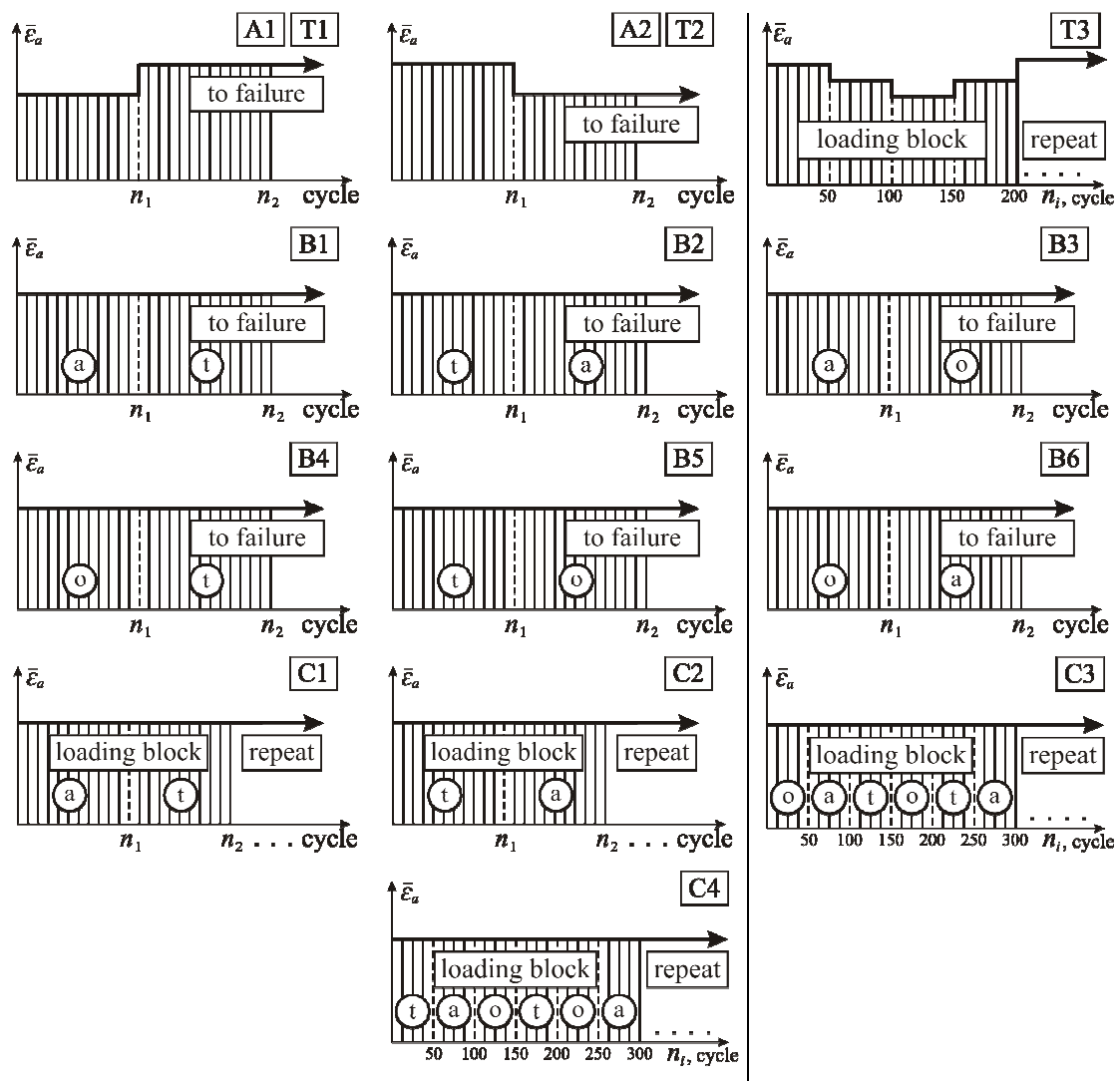


Figure 4. Loading blocks consist of different combinations of axial, torsion, and 90° out-of-phase strain paths

## TEST RESULTS AND ANALYSIS

The test results of two alloys under block loading are presented in Tables 3a and 3b, where  $n_i$  is number of cycles for  $i$ -stage of loading,  $N_f$  is number of cycles till failure.

Table 3a. Block loading test results for BT9 titanium alloy

Loading block	Loading parameters			$N_f$	Loading block	Loading parameters			$N_f$
	$\varepsilon_a$	$\gamma_a/\sqrt{3}$	$n_i$			$\varepsilon_a$	$\gamma_a/\sqrt{3}$	$n_i$	
	%		cycles			%		cycles	
A.1	0.8/1.0	-	157/136	293	C.1	1.0	-	65	510
A.1	0.6/1.0	-	408/124	532		-	1.0	219	
A.2	1.0/0.8	-	98/147	245	C.1	1.0	-	40	423
T.1	-	0.8/1.2	505/187	692		-	1.0	130	
T.2	-	1.2/0.8	213/458	671	C.3	0.8	1.0	50	475
A.3	0.6/0.8/1.0/0.8	-	50	519	C.2	-	1.0	176	457
	1.0/0.8	-	50	491		1.0	-	66	
A.4	1.0/0.8/0.6/0.8	-	50	491	C.2	-	1.0	209	377
T.3	-	0.8/1.0/1.2/1.0	50	601		1.0	-	65	
T.4	-	1.2/1.0/0.8/1.0	50	528	B.1	1.0	-	97	398
						-	1.0	301	
B.5	-	1.0	282	390	B.3	-	1.0	398	603
	1.0	1.0	108			1.0	-	205	
B.6	1.0	1.0	61	131	B.4	1.0	-	98	184
	1.0	-	70			1.0	1.0	86	
						1.0	1.0	80	384
						-	1.0	304	

Table 3b. Block loading test results for BT1-0 titanium alloy

Loading block	Loading parameters			$N_f$	Loading block	Loading parameters			$N_f$
	$\varepsilon_a$	$\gamma_a/\sqrt{3}$	$n_i$			$\varepsilon_a$	$\gamma_a/\sqrt{3}$	$n_i$	
	%		cycles			%		cycles	
A.1	0.7/1.1	-	491/214	705	B.1	0.9	-	228	625
A.2	1.1/0.7	-	104/302	406		-	0.9	397	
A.2	1.0/0.7	-	200/184	384	B.2	-	0.9	434	809
A.1	-	0.7/1.1	1115/242	1357		0.9	-	375	
A.2	-	1.1/0.7	198/805	1003	B.3	0.9	-	228	463
A.2	-	1.1/0.7	198/1253	1451		0.9	0.9	235	
C.4	0.7	0.7	50	1045	B.4	0.9	0.9	138	605
						-	0.9	467	
B.5	-	0.9	428	683	B.6	0.9	0.9	138	293
	0.9	0.9	255			0.9	-	155	

The Figure 5 presents the damage ratios of low-high and high-low axial and torsion loading blocks (A and T blocks) for BT1-0 and BT9 titanium alloys. As can be seen from this figure and Table 3a and 3b no essential effect on fatigue life is observed both materials for torsion blocks and fatigue behavior can be explained by linear damage rule. Therefore, there is no deformation history effect for this case. However, for A1 blocks switching the loading regimes from low-high to high-low is attended by increasing of fatigue life, notably there is effect of “material training”. On the contrary, for A2 block switching the loading from high-low to low-high is attended by reduction of fatigue life.

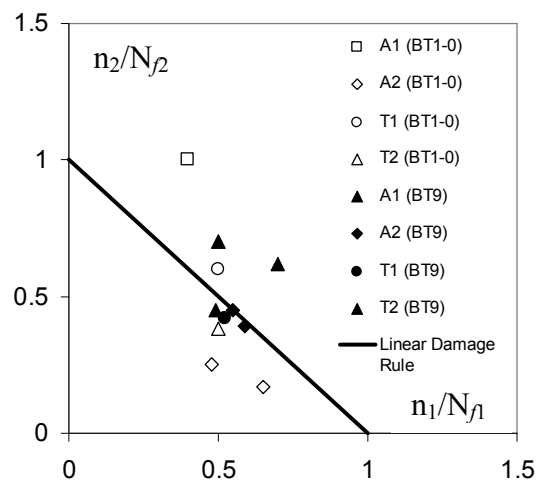


Figure 5. Linear damage ratios of low-high and high-low axial and torsion loading blocks for BT1-0 and BT9 titanium alloys.

As it was obtained from B loading block tests shorter fatigue lives are observed for first applying 90° out-of-phase strain cycles, then either axial or torsion strain cycles, as compared to applying axial or torsion cycles first and then 90° out-of-phase cycles. This can be explained by more possibility of crack initiation under 90° out-of-phase strain path than under axial or torsion cycles.

It was observed increasing of BT9 fatigue life for C1 (axial than torsion cycles) loading block which can be addresses to “material training” effect in comparison with linear damage rule and vice versa for C2 loading block (torsion than axial cycles).

The test results of BT9 titanium alloy under C3 loading block show “material training” effect influences on damage accumulation more considerably.

As opposed to BT9 titanium alloy, it was observed no “material training” effect for C4 loading block of pure titanium, therefore damage accumulation process closes to linear damage rule.

In order to estimate fatigue life for all loading blocks it were examined Miner linear damage rule [3] and Manson-Halford hypotheses [4] in combination with modified Pisarenko-Lebedev strain parameter [5]. Comparisons of observed fatigue lives with the predicted lives by indicated hypotheses of BT1-0 and BT9 titanium alloys are presented

in Fig. 6. As can be seen from this figure, the lowest scatter band of data is observed for non-linear damage rule in form of Manson-Halford. It can be related to non-linear damage accumulation for axial loading blocks and for blocks with significant portion of 90° out-of-phase cycles.

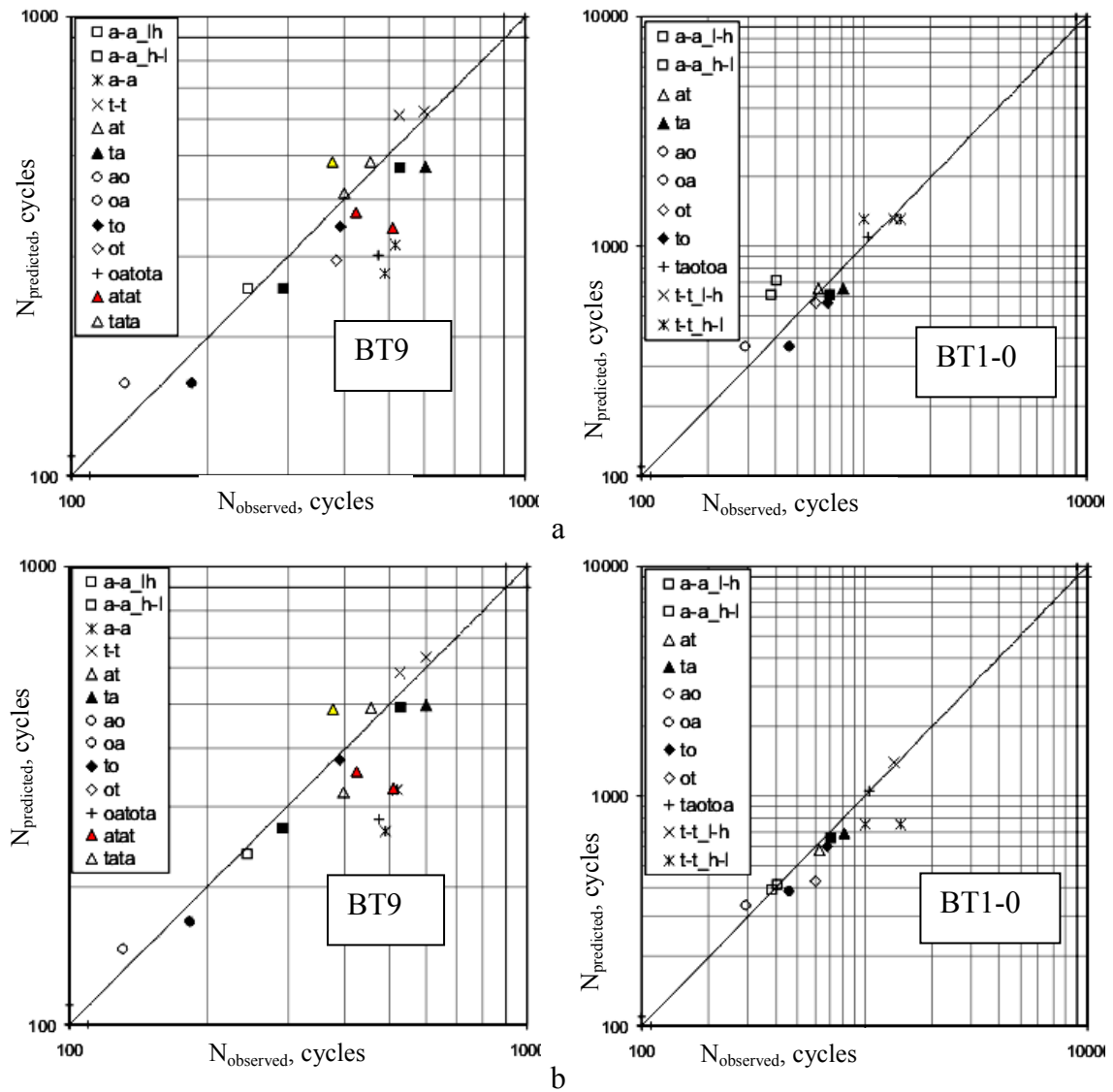


Figure 6. Comparison of observed and predicted fatigue lives by Miner linear damage rule (a) and Manson-Halford hypotheses (b) for all loading blocks of BT1-0 and BT9 titanium alloys.

## CONCLUSION

The block loading test of BT1-0 and BT9 titanium alloys as combinations of axial, torsion, and 90° out-of-phase axial-torsion cycles were conducted to study the effects of over-loading, load path sequence on fatigue behavior. The following conclusions can be made based on the tests and analysis results:

1. Not a significant effect of over-loading or load sequence on fatigue life of BT1-0 and BT9 titanium alloys was observed in this study.
2. Some shorter life is observed for axial loading blocks with different level of von Mises equivalent strain in comparison with the same torsion condition. The damage accumulation under axial block loading has non-linear character and could not be explained by linear damage rule.
3. Shorter fatigue lives are observed for first applying 90° out-of-phase strain cycles, then either axial or torsion strain cycles, as compared to applying axial or torsion cycles first and then 90° out-of-phase cycles.
4. Comparison of linear and non-linear damage rules in combination with modified Pisarenko-Lebedev strain parameter in term of fatigue life prediction show good data correlation by Manson-Halford hypothesis.
5. In order to estimate fatigue life of BT1-0 and BT9 titanium alloys without extra material constant it is necessary to use parameters which are addressed to failure planes, such as critical plane approaches.

## REFERENCES

1. Ukrainian Standard of Design, 1985, "Design, Calculation and Strength Testing. Methods of Mechanical Testing of Metals. Method of Testing on the Low Cycle Fatigue and Heat Mechanical Loading," ГОСТ 25.505-85, In Russian.
2. Shamsaei N., Gladskyi M., Panasovskyi K., Shukayev S., Fatemi A. Multiaxial Fatigue of Titanium Including Step Loading and Load Path Alteration and Sequence Effects, 2010, *Submitted to International Journal of Fatigue*.
3. Miner M.A. Cumulative damage in fatigue. *Journal of Applied Mechanics*, 1945, 67, A159-A164.
4. Manson S.S. and Halford G.R. Practical implementation of the double linear damage rule and damage curve approach for treating cumulative fatigue damage. *International Journal of Fracture*, 1981, 17(2), 169-192.
5. Shukayev S., Gladskyi M., Zakhovayko O., Panasovskyi K. Method for Low-Cycle Fatigue Life Assessment of Metallic Materials under Multiaxial Loading. *Strength of Materials*, 2008, 40(1), 56 - 59.